Inorganic Chemistry

pubs.acs.org/IC Article

Light-Triggered Metal Coordination Dynamics in Photoswitchable Dithienylethene–Ferrocene System

Manisha Karmakar, Adwitiya Pal, Bijan Mondal, Nayarassery N. Adarsh, and Arunabha Thakur*

Cite This: *Inorg. Chem.* 2021, 60, 6086–6098 Read Online

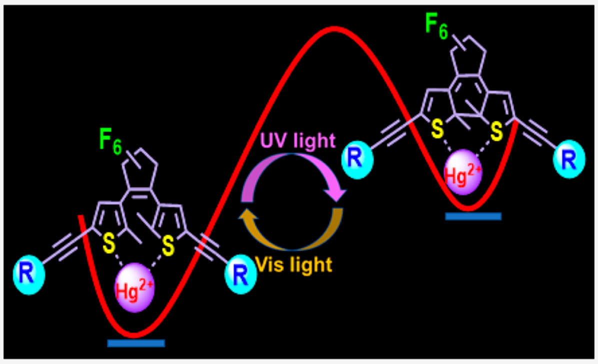

ABSTRACT: The C_2-symmetric photochromic molecule **3**, containing dithienylethene (DTE) and ferrocene units connected by an alkyne bridge, represents a unique probe where a metal (Hg^{2+}) binds with the central DTE moiety. Both photoisomerized states of **3** (open, **3o**; closed, **3c**) are found to interact with Hg^{2+} ion by the S atoms of the DTE core; however, the binding constants (from a UV–vis study) and DFT calculations suggest that the open isomer (**3o**) binds with the metal ion more strongly than that of the closed isomer (**3c**). Notably, the course of metal binding does not perturb the inherent photoisomerization properties of the DTE core and the photoswitchability persists even in the metal-coordinated form of **3**, however, with a comparatively slower rate. The quantum yields for photocyclization ($\Phi_{o\to c}$) and photocycloreversion ($\Phi_{c\to o}$) in the free form are 0.56 and 0.007, respectively, whereas the photocyclization quantum yield in the Hg^{2+} complexed species is 0.068, 8.2 times lower than the photocyclization quantum yield ($\Phi_{o\to c}$) of free **3o**. Thus, the rate of photoisomerization can be modulated by a suitable metal coordination to the DTE core. The dynamics of photoswitchability in the metal-coordinated form of DTE has been explored by experimental means (UV–vis and electrochemical studies) as well as quantum chemical calculations.

INTRODUCTION

Stimuli-responsive organic materials with inherent photoswitchable properties constitute a burgeoning field of research, especially in materials science[1] and structural biology.[2] From the pioneering work of Irie in the late 1980s and early 1990s photochromic diarylethenes (DAE)[3] were primarily associated with dithienylethene (DTE), which undergoes 6*π* electrocyclic ring closing or opening to obtain closed and open isomers under irradiation of UV and visible light, respectively (Scheme 1).[4] The open (o) and closed (c) forms of DTE exist as two distinctly addressable and thermally stable states. They even respond independently to electrochemical and photochemical stimuli.[5] Utilizing its open–closed photoswitchable property in the presence of light, DTE-containing compounds have potential applications in photonic devices: e.g., optical memories and display devices and optoelectronic devices such as waveguides, sensors, etc.[6] Various photochromic metal complexes have also been developed by several research groups for the development of organic optical transistors,[7] NLO switches,[8] organic light-emitting diodes (OLED),[9] energy storage systems (batteries),[10] and many more. Thus, DTE derivatives have been of recent interest due to their wide scope of application.

Scheme 1. Photoisomerization in DAE/DTE Systems

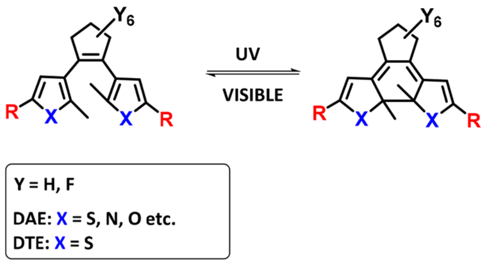

Several research groups have focused on the study of metal-coordinated dithienylethene (DTE) backbones in different fields. A Zn^{2+} bipyridyl complex attached to a DTE core has been utilized in the reversible switching of an NLO response,[11] and a Cu^{+} bipyridyl complex with an appended DTE moiety has been employed in monitoring quadratic NLO properties.[12] Also, Pt terpyridine acetylide complexes with pendant DTE moieties have been used in studying the resultant photophysics where the two components (Pt complex and DTE) have different intramolecular energy transfer processes.[13] Recently,

Received: March 1, 2021
Published: April 8, 2021

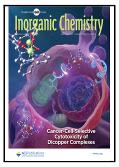

https://doi.org/10.1021/acs.inorgchem.1c00602
Inorg. Chem. 2021, 60, 6086–6098

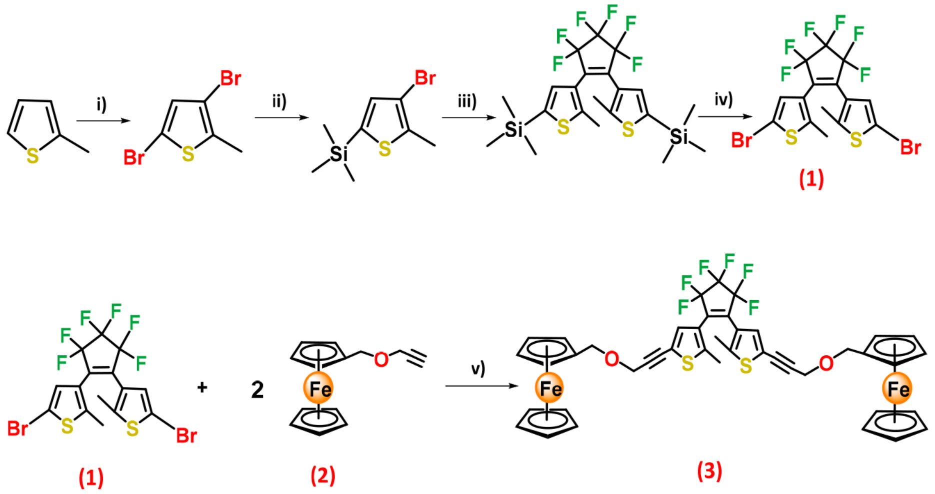

Figure 1. Synthetic route of compound **3**: (i) NBS, glacial AcOH, rt, 2 h; (ii) *n*-BuLi in THF, TMSCl, −78 °C to rt, 12 h; (iii) *n*-BuLi in THF, octafluorocyclopentene, −78 °C to rt, 18 h; (iv) NBS, glacial AcOH, reflux, overnight; (v) $Pd(PPh_3)_4$, CuI, Et_3N, 65 °C, 7 h.

Clever and co-workers have developed coordination cages based on a Pd(II) metal ion and DTE unit, which allow modulation of guest uptake and release by irradiation with light of different wavelengths.[14] Furthermore, there are many examples of chemosensors, based on DTE derivatives,[15] where heteroatoms containing fluorophores are attached to the DTE unit and those heteroatom-containing fluorophores assist or participate in metal coordination.[16] All such probes are designed in a way so that the metal ions do not attach to the sulfur atoms of the DTE core itself and consequently do not intervene directly in the photoisomerization process; rather, they bind with a remote binding unit attached to the DTE core.

In order to explore the coordinating capability of the DTE unit toward metal ions, the design of the molecule should be such that there is a minimal number of other possible binding sites available for the metal ion. Thus, any additional heteroatom-containing fluorophore unit should principally be avoided in the molecular design. In turn, to get access to both thiophene units at a time, an alkyne moiety (ethynylferrocene) could be attached to the DTE unit, as an alkyne group is known to provide linearity in a structure[17] and therefore can impart rigidity and additional stability to the whole structure. On the other hand, ferrocene is a well-established electrochemically responding unit, which gives a pair of reversible waves in voltammetric studies and is stable under moist and aerobic conditions. The DTE unit itself is also electrochemically active by producing irreversible waves,[18] but to get to a conclusive electrochemical study, a standard redox moiety with reversible waves is beneficial for a comparative output. Also, there is a negligible scope of binding by the ferrocene unit, such that it does not compete with the binding experiments of the DTE unit.

Unlike the vast majority of DAE or DTE photochromes containing metal complexes,[14,19,20] our designed compound represents a unique example in which the Hg^{2+} ion directly coordinates to the S atoms of thiophene rings of the photochromic unit, thereby intervening directly in the dynamics of the photoisomerization process. Herein, we have designed and synthesized the molecule **3**, devoid of any additional binding site or fluorophore, and it was utilized to evidence the binding activity of the DTE core itself with the soft Hg^{2+} ion, in both its open (**3o**) and closed (**3c**) forms for the first time. In this study we are able to show that the photoisomerization in the DTE core remains unhindered but is decelerated upon binding with an Hg^{2+} ion in the same unit.

■ RESULTS AND DISCUSSION

Synthesis and Characterization. The synthesis of the target symmetrical ferrocene-based DTE moiety connected via an alkyne bridge is designed as depicted in Figure 1. In the design of our molecular architecture, we wish to combine the photochromic unit (DTE) with a redox-active ferrocene moiety via an alkyne (C≡C) bridge, anticipating that the alkyne (C≡C) bridge may impart rigidity to the molecule. However, a Sonogashira coupling between the diiodo DTE derivative (I-DTE-I) and ethynylferrocene in the presence of $Pd(PPh_3)_4$ and CuI is known to produce the di-1,4-ferrocenylbutadiyne ("Glaser product") by homocoupling of ethynylferrocene as a byproduct along with the desired product (by Sonogashira coupling).[21] Therefore, to minimize the self-coupling reaction and to yield the Sonogashira product as the only product, we have introduced the $CH_2{-}O{-}CH_2$ functionality as a spacer between the terminal alkyne group and the ferrocene unit. This derivatization was expected not to promote the "Glaser" coupling reaction, and indeed it led to the formation of a Sonogashira coupling product (**3**) as the sole product in good yield. Compound **3** was obtained as a bright yellow solid in 85% yield by a Sonogashira cross-coupling reaction between Br-DTE-Br (**1**) and ferrocene-3-ethoxyprop-1-yne (**2**), in the presence of $Pd(PPh_3)_4$ catalyst, CuI cocatalyst, and Et_3N base at 65 °C (Figure 1 and Figure S1). The molecule **3** was fully characterized by ^1H, ^{13}C, and ^{19}F NMR, HRMS, IR spectra and elemental analysis. Additionally, the molecular structure of compound **3** was unambiguously established by a single-crystal diffraction analysis (Figure 2a). **3o** crystallizes in the triclinic space group $P\bar{1}$. In the crystal structure, the compound undergoes intermolecular hydrogen bonding through C−H of the ferrocene and an F atom present in the backbone moiety (C−H···F = 3.248(10) Å, ∠C−H−F = 126.88°), resulting in a two-dimensional hydrogen-bonded porous network (Figure 2b). The 2D sheets are further assembled on top of each other through various van der Waals interactions (Figure 2c).

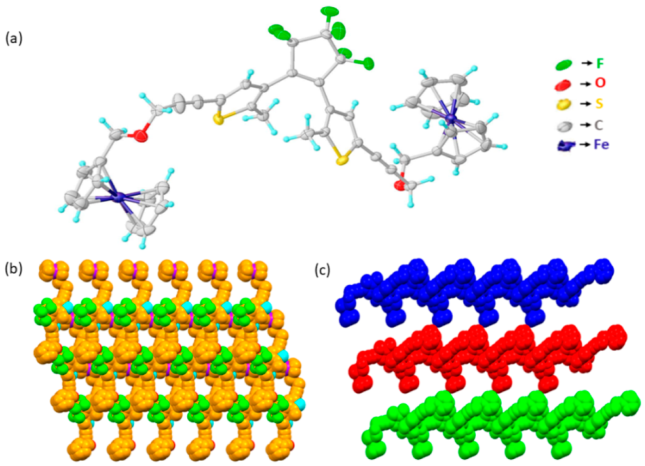

Figure 2. (a) X-ray structure of **3o** drawn with thermal ellipsoids at the 50% probability level. (b) Porous 2D hydrogen-bonded network structure. (c) Parallel packing of the 2D networks sustained by van der Waals interactions.

Our objective for synthesizing compound **3** was not to utilize this molecule as a selective sensing probe for a particular metal ion; rather, we were interested in monitoring the change in photoswitching efficiency upon coordination of any metal ions to the core DTE unit, anticipating some influence on the dynamics of photoswitching if any metal ions coordinate directly to the DTE core. However, we have screened several metal ions (Fe^{3+}, Zn^{2+}, Cu^{2+}, Fe^{2+}, Hg^{2+}, Pb^{2+}, Ag^{+}, Co^{2+}, Ni^{2+}, Pd^{2+}, Cu^{+}, and Cd^{2+}) to check the binding affinity and coordination behavior toward the S atoms of the DTE unit and control the chemistry of photoswitching. Addition of all the aforementioned metal ions, even in large excess, in CH_3CN solution to the receptor **3** did not impart any color changes visible to the naked eye except for Hg^{2+}, Fe^{3+}, and Cu^{2+} ions (Figure S8a). Interestingly, for the sake of comparison, we have also screened compound **1** as a reference, containing the S atoms of DTE, with all the aforementioned metal ions, anticipating the type of interaction similar to that of compound **3**. However, no color change of a colorless acetonitrile solution of **1** (10^{-3} M) in the presence of any of the same series of metal ions (Figure S8b) could be observed by the naked eye (Figure 3a), which would usually occur for any kind of interaction between two species. Further, the absence of any such interaction was validated by UV–vis and electrochemical studies, which indicate no changes upon interaction of any of the aforementioned metal ions, including the Hg^{2+} ion, with compound **1** (*vide supra*, Figures S9–S11). Therefore, the inclusion of ferrocene into the design of molecule **3** is necessary as well as beneficial, because it not only serves as an internal standard in voltammetric studies but also acts as a chromogenic unit, giving a vivid colorimetric response from pale yellow to blue (10^{-3} M CH_3CN solution) upon interaction with the Hg^{2+} ion (Figure 3b). The color change perceptible to the naked eye upon metal coordination to the DTE moiety is always advantageous to comprehend the photoswitching dynamics of a metal-chelated DTE moiety more rapidly. The noninteractive nature of compound **1** may be due to the strong electron-withdrawing property of the two bulky Br atoms, rendering the S atoms of DTE unit less nucleophilic, and may generate steric hindrance to accommodate the Hg^{2+} ion.

UV–Vis Absorption Study. The photochromic DTE unit gives rise to some characteristic undulations in the UV–vis spectra.[21] The UV–vis spectra of many compounds containing the DTE unit have been reported in the literature; however, each new orientation of atoms results in a unique property. The synthesized molecule **3o** was designed with the intention of investigating the reversible photoswitching behavior of the DTE unit in the presence of chelating metal ions. To investigate the behavioral absorption fingerprint in our designed architecture, **3o** was exposed to UV irradiation having a monochromatic wavelength of 365 nm and to visible light.

As shown in Figure 4a, **3o** displayed an absorption peak at 263 nm ($\varepsilon = 3.66 \times 10^3\ M^{-1}\ cm^{-1}$) due to a $\pi-\pi^*$ transition in the open form.[22] The irradiation of 365 nm UV light for the transformation from **3o** to **3c** was done periodically with 5 s of irradiation time, and the consequent UV–vis spectra were recorded. When a CH_3CN solution of **3o** (3 mL, 5×10^{-5} M) was periodically irradiated by 365 nm UV light for 5 s, the 263 nm peak showed a slight increment in intensity, whereas a new shoulder peak at 581 nm ($\varepsilon = 3.01 \times 10^2\ M^{-1}\ cm^{-1}$), characteristic of the closed DTE unit,[23] appeared. The peak intensified with gradual irradiation, and after 5 min (300 s) of irradiation, saturation was obtained, signifying almost full conversion from **3o** to **3c**, accompanied by a color change to violet from pale yellow (Figure 5).

In order to investigate the metal-chelation ability of **3o** and **3c** along with the dynamics of the phototransformation from **3o** to **3c** in free and metal-chelated forms, the interactions of **3o** with several metal ions were investigated by UV–vis spectra (Figure S12). Only Hg^{2+}, Fe^{3+}, and Cu^{2+} ions displayed positive responses, among which the responses produced by Fe^{3+} and Cu^{2+} ions originate from the oxidation of ferrocene (Fe^{2+}) to ferrocenium ion (Fe^{3+}), the formation of which was confirmed by the appearance of a new characteristic absorption

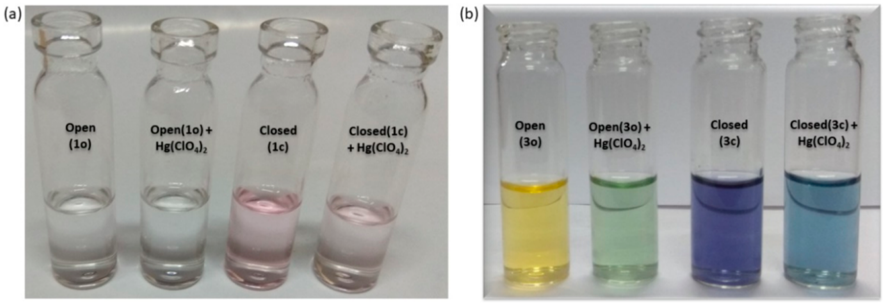

Figure 3. Visible color changes of (a) **1** (open and closed) and (b) **3** (open and closed) in the presence of $Hg(ClO_4)_2$ in 10^{-3} M CH_3CN solution.

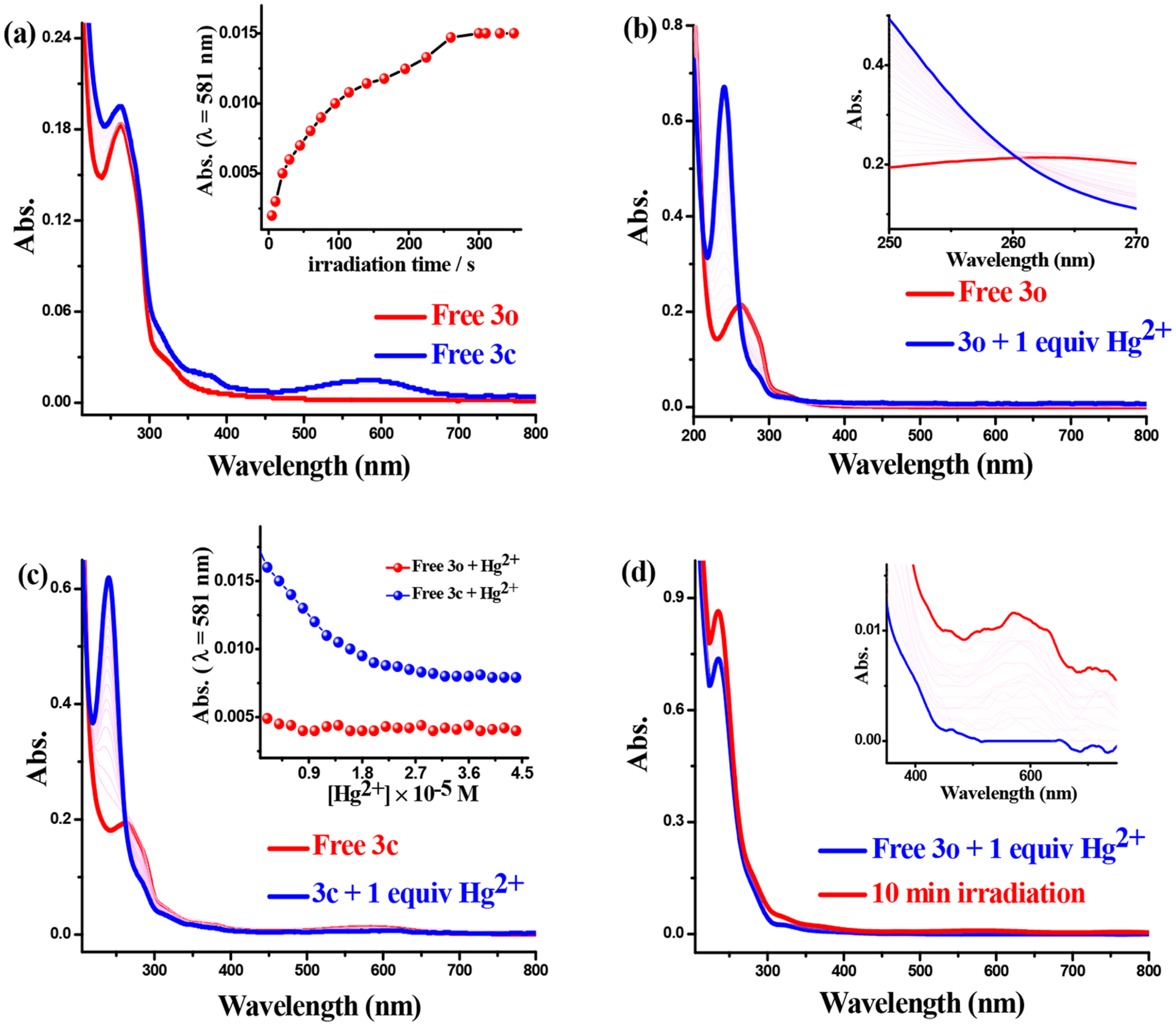

Figure 4. (a) Changes in the absorption spectra of **3o** by gradual irradiation with 365 nm UV light in CH_3CN (inset: variation of absorption intensity at 581 nm against irradiation time, upon transforming from **3o** to **3c**). (b) Changes in the absorption spectra of **3o** (5×10^{-5} M) upon gradual addition of Hg^{2+} ion up to 1 equiv in CH_3CN solvent (inset: enlarged portion representing the isosbestic point at 259 nm). (c) Changes in the absorption spectra of **3c** upon gradual addition of Hg^{2+} up to 1 equiv (inset: variation of absorption intensity of **3c** at 581 nm with [Hg^{2+}] and its comparison with **3o** for the same). (d) Changes in the absorption spectra of [**3o**·Hg^{2+}] upon irradiation with 365 nm UV light (inset: enlarged portion representing the emergence of a peak at 581 nm).

peak at around 630 nm[24] (Figure S13). The back-reduction of the oxidized ferrocenium ion (Fe^{3+}) to ferrocene (Fe^{2+}) again was also achieved by adding sodium L-ascorbate, a reducing agent, to the acetonitrile solution of the oxidized species, indicating the reversible oxidation−reduction nature of the interaction (Figure S14). On the other hand, the Hg^{2+} ion did not promote any such redox interaction; rather, it induced the formation of a complex with **3o** and **3c**. Therefore, the interactions of **3o** and **3c** with Hg^{2+} were carefully monitored to execute a study of the phototransformation in the metal-chelated form. Upon stepwise addition of Hg^{2+} ion (5×10^{-5} M) up to 1 equiv in CH_3CN solutions of **3o** (5×10^{-5} M) (Figure 4b) and **3c** (5×10^{-5} M) (Figure 4c) separately, the absorption maximum at 263 nm decreased in intensity with the emergence of a new peak at 240 nm (Figure S15). Two distinct isosbestic points at 211 and 259 nm appeared for **3o** along with a color change from pale yellow to blue (Figure 5). However, no well-defined isosbestic point was obtained for **3c**, and the band at 581 nm diminished slightly by Hg^{2+} addition, along with a change in color of the solution from violet to green (Figure 5). Binding stoichiometries of 1:1 were determined for both **3o** and **3c** with the Hg^{2+} ion from Job's plot (Figure S16) and elemental analysis. Binding constant values of **3o** and **3c** with Hg^{2+} were determined from the equation[25] $1/[A - A_0] = 1/K(A_{max} - A_0)[Hg^{2+}]_n + 1/(A_{max} - A_0)$, where, A_{max} is the maximum absorbance; A_0 is the initial absorbance of free ligand (**3**) and A is the absorbance after addition of Hg^{2+}. The binding constant (K) values for both isomers (**3o** and **3c**) are 4.779×10^4 and 2.149×10^4 M^{-1} ($\log K = 4.679$ and 4.332 for **3o** and **3c**), respectively (Figure S17), indicating a slightly stronger binding (2.22 times) of **3o** with Hg^{2+} in comparison to **3c**: i.e., this suggests that **3c** is a weaker

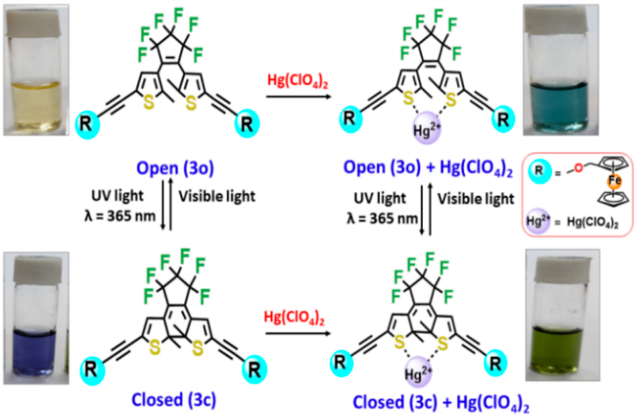

Figure 5. Schematic representation of the photoresponsive switching process of **3o** and **3c** in the presence of Hg(ClO$_4$)$_2$ and lights of different wavelengths.

competitor than **3o** for binding with Hg^{2+}. To elucidate the efficiency of electrocyclization and cycloreversion, quantum yield calculations were performed. The quantum yields for photocyclization ($\Phi_{o\rightarrow c}$) and cycloreversion ($\Phi_{c\rightarrow o}$) of **3** were found to be 0.56 and 0.007, respectively (Figure S18 and Table S3), in hexane with 1,2-bis(2-methyl-5-phenyl-3-thienyl)-perfluorocyclopentene as a reference.[26] The quantum yield was evaluated from the equation

$$\Phi(\mathbf{3}) = \left(\frac{\mathrm{slope}(\mathbf{3})}{\mathrm{slope}(\mathrm{ref})}\right) \times \left(\frac{\varepsilon(\mathrm{ref})}{\varepsilon(\mathbf{3})}\right) \times \Phi(\mathrm{ref})$$

where slope is the slope of the linear plot, extracted from A (absorbance) vs t (irradiation time) plot, ε is the molar extinction coefficient of the concentration 5×10^{-5} M at 574 nm for the reference and at 581 nm for **3**, and Φ is the quantum yield.

Moreover, in order to investigate the open to closed isomerization process in the metal-chelated form, a CH$_3$CN solution of [**3o**·Hg^{2+}] was subjected to UV irradiation (λ = 365

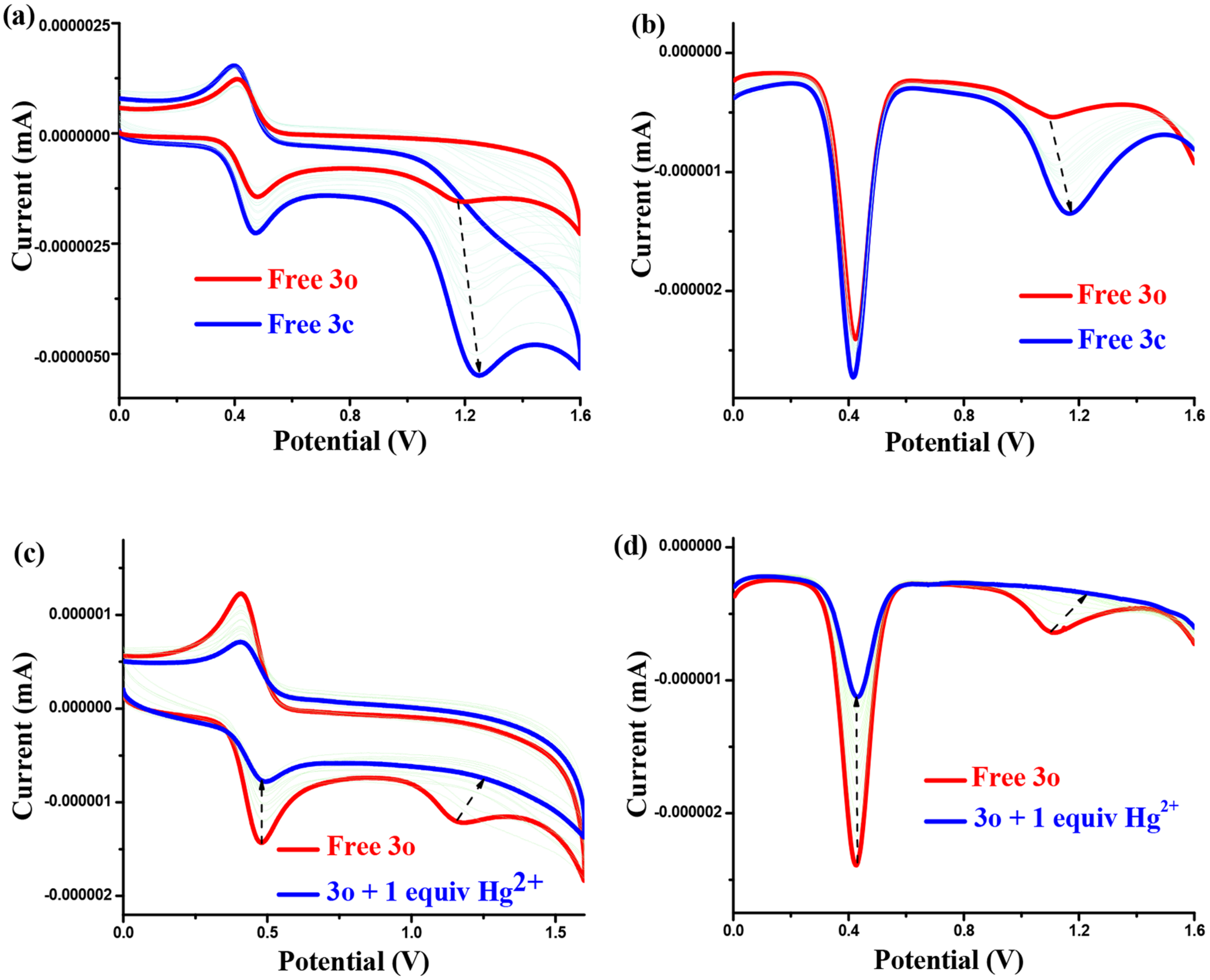

Figure 6. (a) Cyclic voltammetry (CV) and (b) differential pulse voltammetry (DPV) of the open form (**3o**) to closed form (**3c**) upon UV irradiation (λ = 365 nm). (c) Cyclic voltammetry (CV) and (d) differential pulse voltammetry (DPV) of **3o** (open form) upon addition of Hg^{2+} up to 1 equiv in CH$_3$CN solution with [(n-Bu)$_4$N]ClO$_4$ as the supporting electrolyte at a 0.06 V s^{-1} scan rate.

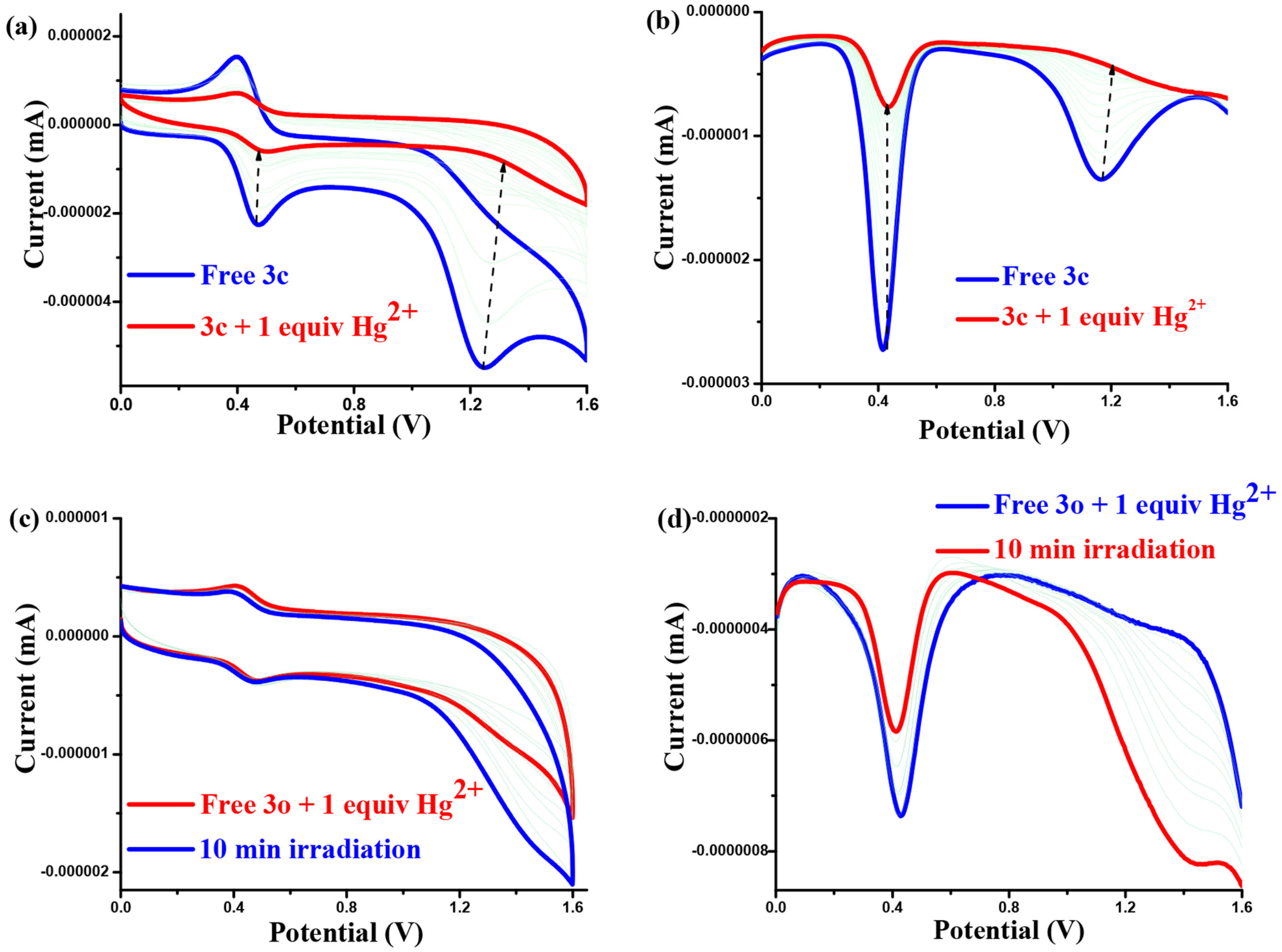

Figure 7. (a) Cyclic voltammetry (CV) and (b) differential pulse voltammetry (DPV) of **3c** (closed form) upon addition of Hg^{2+} up to 1 equiv. (c) Cyclic voltammetry (CV) and (d) differential pulse voltammetry (DPV) of [**3o**·Hg^{2+}] upon UV irradiation (λ = 365 nm) in CH_3CN solution with $[(n\text{-Bu})_4N]ClO_4$ as the supporting electrolyte at a 0.06 V s^{-1} scan rate.

nm), with 5 s intervals (Figure 4d). The characteristic band for **3c** at 581 nm ($\varepsilon = 4.36 \times 10^2$ M^{-1} cm^{-1}) appeared after 15 s of irradiation of the [**3o**·Hg^{2+}] complex, whereas it appeared after 5 s for free **3o**. The band at 240 nm ($\varepsilon = 26.91 \times 10^3$ M^{-1} cm^{-1}), which appeared due to the interaction of **3o** with Hg^{2+}, remained unperturbed even after irradiation of [**3o**·Hg^{2+}] for a long time, and the formation of peak at 581 nm is very slow for the [**3o**·Hg^{2+}] solution. This slower kinetics of ring closing in the metal-chelated form, [**3o**·Hg^{2+}], was also supported by the lower (8.2 times) quantum yield ($\Phi_{o\rightarrow c}$) of 0.068 (Figure S18 and Table S3), in comparison to that of free **3o**. This shows that, although [**3o**·Hg^{2+}] gets converted to [**3c**·Hg^{2+}], the rate of conversion[27] of free **3o** to **3c** ($k = 0.01$ s^{-1}) is faster than the rate of conversion of [**3o**·Hg^{2+}] to [**3c**·Hg^{2+}] ($k = 0.007$ s^{-1}), as is also confirmed by kinetic studies, using UV−vis spectra (Figure S19). The binding equilibrium in **3c** is not being as stable as that for the open isomer may be due to the formation of a strained and puckered five-membered C−S−Hg−S−C ring, as indicated by DFT calculations (*vide infra*).

In order to assess the kind of interaction (in terms of reversibility) between **3o**/**3c** and Hg^{2+}, an aqueous solution of Na_2EDTA (5×10^{-5} M) was employed as a decomplexing agent into the corresponding CH_3CN solution. The nature of the interaction of both **3o** and **3c** with Hg^{2+} is reversible: i.e., with every aliquot of Na_2EDTA addition to a CH_3CN solution of the [**3o**/**3c**·Hg^{2+}] complex, the UV−vis spectrum corresponding to free **3o**/**3c** was generated, whereas upon Hg^{2+} addition to the same solution, the UV−vis spectrum corresponding to [**3o**/**3c**·Hg^{2+}] was regenerated. This experimental cycle could be repeated two times without much loss of sensitivity; however, in the third cycle the sensitivity decreased slightly (Figure S20).

Electrochemical Studies. To realize the changes occurring in DTE derivatives in the presence of metal ions by electrochemical studies was one of the principal objectives of including a ferrocene unit within the core of the designed molecule. The electrochemically reversible behavior of ferrocene[28] and irreversible nature of dithienylethene[29] in **3o** was observed in cyclic voltammetry (CV) and differential pulse voltammetry (DPV) experiments, which were carried out at room temperature in CH_3CN solution (1.25×10^{-4} M) containing 0.1 M $[(n\text{-Bu})_4N]ClO_4$ (TBAP) as the supporting electrolyte.

To start the electrochemical studies, the CV of **3o** was recorded, which displayed a reversible oxidation wave at 0.426 V corresponding to the ferrocene/ferrocenium couple[30] and an irreversible wave at 1.11 V characteristic of the dithienylethene (DTE) core.[31] Upon UV irradiation of **3o** by 365 nm light, an

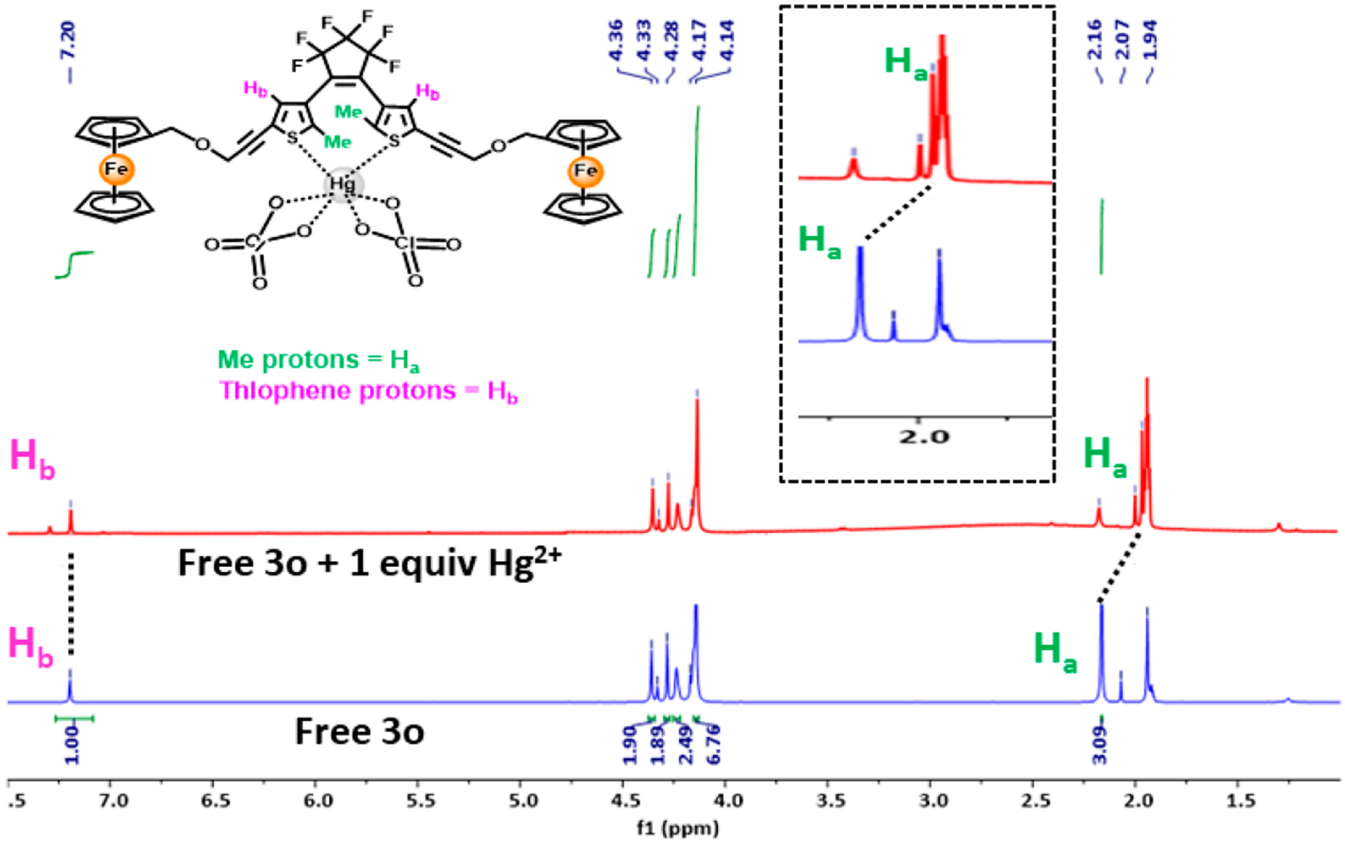

Figure 8. Comparative ^{1}H NMR spectra of **3o** in the presence of 1 equiv of Hg^{2+} in CD_3CN as a solvent.

increment of the irreversible wave at 1.11 V was observed along with a slight anodic shift to 1.16 V ($\Delta E_{1/2}$ = 50 mV), which marked the transformation of **3o** to **3c** (Figure 6a,b). The increment of intensity of the irreversible wave upon **3o** to **3c** conversion may be attributed to the fact that the closed form is electrochemically more active than the open DTE core.[32]

An acetonitrile solution of Hg^{2+}(1.25×10^{-4} M) was added stepwise into CH_3CN solutions of **3o** and **3c** separately, to conduct binding studies using an electrochemical method. The oxidation wave at 0.426 V for both **3o** (Figure 6c,d) and **3c** (Figure 7a,b) did not exhibit any shift in potential, whereas the peaks at 1.11 and 1.16 V respectively shifted anodically to 1.17 and 1.19 V ($\Delta E_{1/2}$ = 60 and 30 mV), respectively, and became flattened with the gradual addition of Hg^{2+} ion up to 1 equiv. The significant perturbation of the DTE oxidation wave upon Hg^{2+} addition supports the possibility of interaction of **3o** and **3c** with Hg^{2+} by the DTE core. In **3o**, the wave flattened readily after addition of a small amount of Hg^{2+} ion, but in **3c**, the restoration of its own property exceeds the effect of Hg^{2+} binding for up to a large quantity of Hg^{2+} ion. The retainment of the nature of the oxidation wave of DTE core of **3c** until quantitative addition of Hg^{2+} ion proved the sluggish interaction of **3c** in comparison to **3o** with Hg^{2+} ion.

Upon irradiation of the [**3o**·Hg^{2+}] complex with 365 nm UV light (gradually up to a total of 10 min), a substantial difference in the irreversible oxidation wave was observed. The irreversible wave, which had almost flattened due to complexation, was regenerated, but in an indistinct way and to a much lesser extent (Figure 7c,d). This clearly signifies the resistance to the conversion of the open form to the closed form in the presence of a bonded Hg^{2+} ion, which is consistent with other experimental results and DFT calculations. In all of the above experiments, the ferrocene/ferrocenium oxidation wave remained almost undisturbed. A tabular depiction of data (Table S4) and normalized electrochemical measurements (Figure S21) present the changes more clearly, supporting the anticipation of participation of S atoms of the DTE core in both [**3o**·Hg^{2+}] and [**3c**·Hg^{2+}] complexes.

Comparative ^{1}H NMR and IR Studies. The ring-closure process was further monitored by ^{1}H NMR study, which indicated the complete conversion of the open form to the closed form upon irradiation. ^{1}H NMR was studied thoroughly to explore the photoisomerization process as well as the chelation phenomenon. Upon conversion of **3o** to **3c**, in CD_3CN, the characteristic singlet peak for methyl protons shifted downfield (from 2.16 to 2.21 ppm) and the signal assigned to thienyl protons remained unchanged (Figure S7).

To confirm the plausible binding mode of **3o** with Hg^{2+}, ^{1}H NMR spectra were recorded in CD_3CN solution. The spectral changes of **3o** and [**3o**+ 1 equiv Hg^{2+}] are depicted in Figure 8. They exhibited a singlet at 2.16 ppm which corresponds to Me protons, peaks at around 4.14 and 4.36 ppm for substituted ferrocene ring protons and OCH_2, respectively, and another singlet for the aromatic ring proton of the thiophene ring. The Me protons (H_a), close to coordinating S atoms, shifted upfield[33] from 2.16 to 1.96 ppm ($\Delta\delta$ = 0.20 ppm), whereas no such displacement was observed for ferrocenyl (Fc), $-OCH_2$, and thiophene ring (H_b) protons. Hence, the plausible binding mode in **3o** for Hg^{2+} (soft acid) is via S atoms (soft base) present in the DTE unit. After the addition of excess Hg^{2+}, no further change indicated a 1:1 binding stoichiometry. These

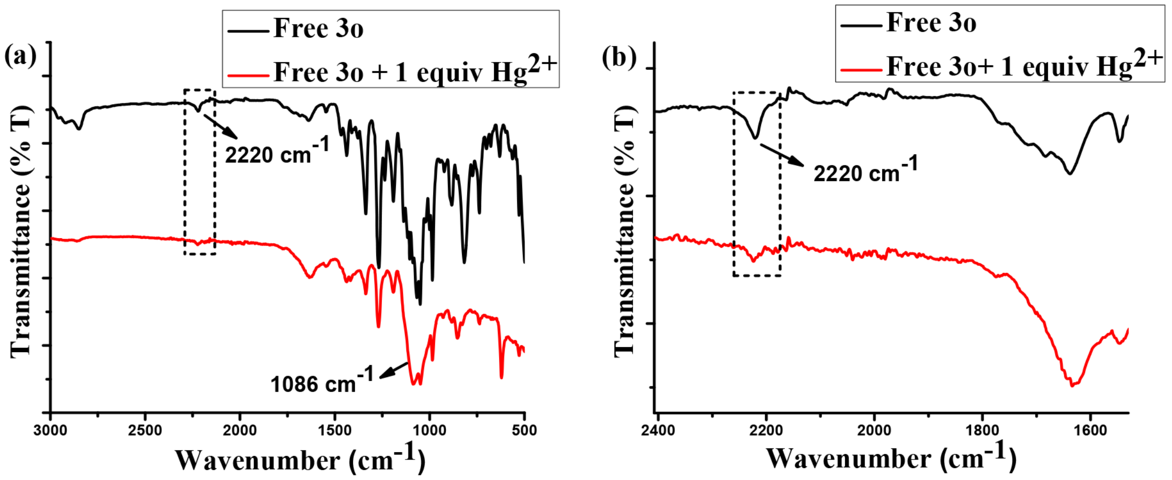

Figure 9. (a) Comparative IR spectra of **3o** in the presence of 1 equiv of Hg^{2+} in the solid state at room temperature. (b) Enlarged image of IR stretching of the alkyne (−C≡C−) peak of **3o** before and after addition of $Hg(ClO_4)_2$.

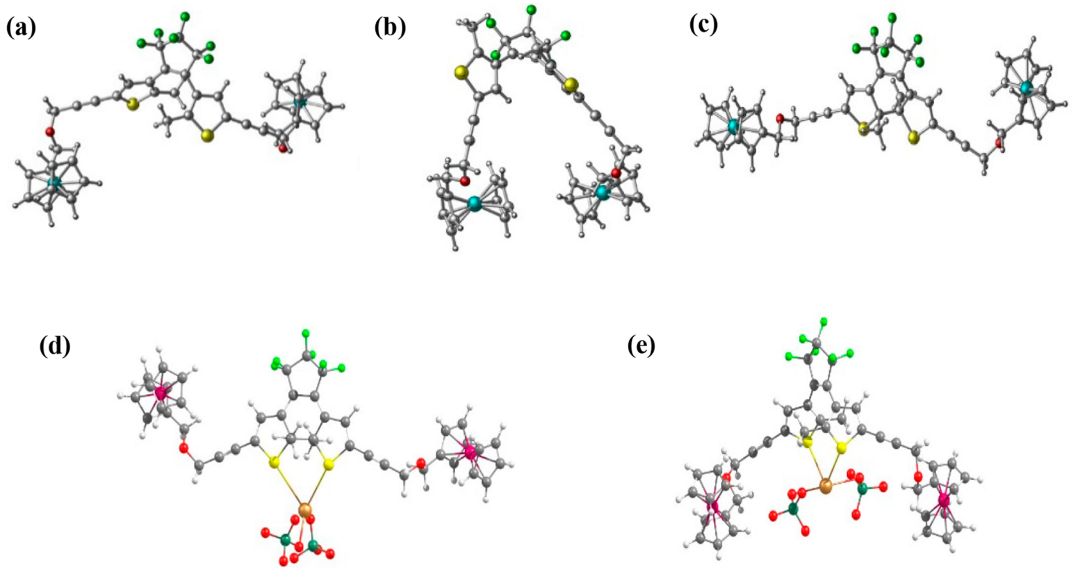

Figure 10. Energy-minimized structures of **3o** ((a) antiparallel and (b) parallel), (c) **3c**, (d) [**3o**·$Hg(ClO_4)_2$], and (e) [**3c**·$Hg(ClO_4)_2$].

results suggest that **3o** may chelate with Hg^{2+}(soft acid) using S atoms (soft base) present in the DTE unit and ferrocene units do not participate in the binding mechanism. This result also corroborates the CV and DPV studies.

In order to get further details about the binding behavior, IR spectra were recorded with Hg^{2+} (as its perchlorate salt). The IR spectra of free **3o** and [**3o** + 1 equiv Hg^{2+}] were measured in the solid state (Figure 9). On addition of $Hg(ClO_4)_2$, the peak at 2220 cm^{-1}, which was assigned to the C≡C stretching frequency,[34] remained unperturbed and a strong band at 1086 cm^{-1} due to Cl−O stretching[35] appeared, indicating the inclusion of $Hg(ClO_4)_2$ unit in **3o** (see the IR sample preparation below). The above observation indicates that the alkyne (C≡C) unit does not participate in coordination to Hg^{2+}, probably due to the adjacent OCH_2 groups which make the alkyne units less susceptible to react with Hg^{2+} ion in comparison to the S atoms. Thus, ^1H and IR titrations come together in unison to suggest a plausible binding mode where **3o** coordinates Hg^{2+} through the S atoms of the DTE core.

Theoretical (DFT) Studies. Solution-phase theoretical calculations were carried out on the ground of density functional theory (DFT) in order to understand the structural and electronic parameters. The coordinates of the starting geometry of **3o** (Figure 10a) were taken from those of the solid-state structure (Figure 2a). However, **3c** (Figure 10c) was derived from the optimized geometry of **3o**. Various starting points of [**3o**·$Hg(ClO_4)_2$] and [**3c**·$Hg(ClO_4)_2$] were finally converged, which led us to conclude their minimized conformation (Figure 10d,e, respectively).

In Figure 10, we have reported the energy-minimized conformers for the parallel and antiparallel forms of the open and closed forms of compound **3**. As was determined, in the antiparallel form (Figure 10a) the ferrocene-containing arms are well separated. The situation is similar in the closed structure **3c** (Figure 10c) ,which is 66.2 kJ/mol less stable than the antiparallel open form **3o** (Table S5). The energy values are consistent with the easy conversion from closed to open conformers. This is also supported by a low energy barrier of 61.6 kJ/mol computed for the closed to open process. This energy difference between the antiparallel open and closed isomers in DTE photochromes is expected.[36] Further, the newly formed elongated C−C bond of 1.548 Å suggests **3c** to be an unstable product.[37] Nevertheless, topological analyses of the frontier orbitals reveal that the LUMO of **3o** indeed has a bonding character between the two reactive C atoms that indicates the possible formation of the closed product **3c**. Notably, the parallel conformer (Figure 10b) is nearly isoenergetic with the antiparallel open form and is unstable by only 4.06 kJ/mol with respect to the antiparallel open conformer (this difference, smaller than 4.2 kJ/mol, is negligible at this level of theory). Therefore, in solution, **3o** exists as a blend of parallel and antiparallel conformers. However, the energy-minimized geometry of **3o** shown in Figure 10a, which is the antiparallel open form, corresponds to the SCXRD structure (Figure S22).

The optimized geometries reveal that the free ligands maintain their core geometries even after binding with the analyte, Hg^{2+}. The optimized geometries of [**3o**·Hg(ClO$_4$)$_2$] and [**3c**·Hg(ClO$_4$)$_2$] show that in both cases Hg^{2+} adopts a distorted-tetrahedral geometry by connecting to two S and two O atoms. Although the S atoms of the DTE core in the molecules **3o**/**3c** are taking part in the interactions with the Hg^{2+} ion, the Hg−S bonds are relatively weak[38] (Wiberg bond index values of ca. 0.2), as evidenced from their Hg−S bond lengths (in [**3o**·Hg(ClO$_4$)$_2$] 3.75, 3.69 Å; in [**3c**·Hg(ClO$_4$)$_2$] 3.71, 3.69 Å). Notably, [**3c**·Hg(ClO$_4$)$_2$] is unstable by 79.3 kJ/mol with respect to [**3o**·Hg(ClO$_4$)$_2$]. Further, the computed energy of the reaction suggests that the complexation of **3o** to Hg^{2+} is 4.7 times more exergonic (−22.7 kJ/mol) than the formation of the complex [**3c**·Hg(ClO$_4$)$_2$] (−4.8 kJ/mol). The calculations also suggest a dynamic coordination process that exists in the solution phase (Figure 11). The results suggest that [**3c**·Hg(ClO$_4$)$_2$] either may convert into free **3o** by releasing Hg^{2+} (which can further combine into [**3o**·Hg(ClO$_4$)$_2$]) or may convert directly into the [**3o**·Hg(ClO$_4$)$_2$] ("**3o**-Hg^{2+}") complex through intramolecular ring opening. This further shows the instability of the [**3c**·Hg(ClO$_4$)$_2$] complex, suggesting a low possibility for the formation of the complex.

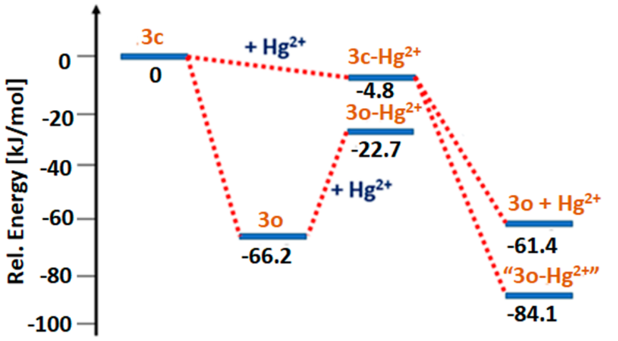

Figure 11. Energy diagram of the reaction of **3c**/**3o** with Hg^{2+}, calculated at the B3LYP/6-31(d,p)LANL2DZ level of theory.

The DFT-calculated MO analyses revealed that, due to extension in plane conjugation, the LUMO of **3c** is stabilized by 1.11 eV in comparison to that of **3o** (LUMO: −1.82 eV (**3o**) and −2.92 eV (**3c**)). This causes a decrease in the HOMO−LUMO gap in **3c**, suggesting a red shift in the absorption spectra (Figures S23−S25); however, no shifts were observed experimentally. The complex formation between **3o** and Hg^{2+} resulted in destabilization of the HOMO of [**3o**·Hg(ClO$_4$)$_2$] by 0.97 eV that also resulted in a decrease in the HOMO−LUMO gap in [**3o**·Hg(ClO$_4$)$_2$], whereas the frontier molecular orbital energies in **3c** and [**3c**·Hg(ClO$_4$)$_2$] are nearly comparable.

To get more information about the electronic transitions, TD-DFT (CAM-B3LYP) calculations have been performed on both the free ligands and the complexes in the solution phase (acetonitrile). The TD-DFT calculations on **3o** show that the $S_0 \rightarrow S_1$ transitions have a large oscillator strength (f = 1.28) (Figure S24 and Table S6) and the excitation wavelength to the S_1 state is calculated to be 267 nm (Table S6). This encompasses the transitions between HOMO-5 to LUMO+1 and HOMO-4 to LUMO+2. These are mainly of ligand to ligand charge transfer (LLCT) character that is mainly centered on the ethynyl and thiophene moieties. On the other hand, the calculated transition at 288 nm for [**3o**·Hg(ClO$_4$)$_2$] (Figure S26, and Table S6) involves two major transitions of MLCT (n(Fe) → π*(C_5F_6 ring)) and LLCT character (π orbital centered on ethynyl and thiophene to π* of the C_5F_6 ring). Calculations on **3c** showed that the excitation wavelengths to the S_1 state are at 302, 344, and 553 nm with oscillator strengths of 0.2, 0.17, and 0.49, respectively (Figure S25 and Table S6). The transition at 344 nm is due to an Fe-based lone pair to the delocalized π* orbital of the ligand (MLCT character), and the transitions at 302 and 553 nm are due to $\pi \rightarrow \pi^*$ transitions of the central part of the ligand (LLCT character). The TD-DFT calculation on [**3c**·Hg(ClO$_4$)$_2$] showed two major transitions to S_1, calculated to be 697 and 572 nm, which are due to a ligand-based $\pi \rightarrow \pi^*$ transition and a ligand-based π → empty orbital centered on Hg, respectively (Figure S27 and Table S6).

■ CONCLUSIONS

In conclusion, we have reported an unprecedented protocol where the coordination strength of a metal ion can discriminate the photoswitchable states of a DTE unit via a simple naked-eye color change and electrochemical analysis; all of the experimental results were further supported by DFT calculations. Moreover, from the dynamics study in terms of quantum yield and rate constants, it can be established that metal coordination slows down the inherent photoswitchable nature of the DTE core. The electrochemical studies by CV and DPV emphasizes the differential responses of the open and closed isomers of **3** toward Hg^{2+}, as well as the effect of metal chelation on photoinduced transformations. The inclusion of a rigid alkyne moiety and a chromogenic ferrocene unit seems to be crucial for the successful practical application of this type of metal-chelated photocontrolled probe. We believe that such fine tuning by metal chelation and the suitable design of DTE-based molecular architecture may open up a new avenue for the development of photocontrolled metal-coordinating smart molecular switches.

■ EXPERIMENTAL SECTION

Materials and Measurements. Unless mentioned otherwise, all of the analytes used for synthesis were purchased from commercially available suppliers and used without further purification. Perchlorate salts of metals (Zn^{2+}, Fe^{2+}, Fe^{3+}, Pb^{2+}, Hg^{2+}, Ag^{+}, Cu^{2+}, Ni^{2+}, Pd^{2+} and Cd^{2+}), $CoCl_2\cdot 6H_2O$, and $[Cu(CH_3CN)_4]PF_6$ were purchased from Sigma-Aldrich. K_2CO_3, NBS, and glacial acetic acid were purchased from local chemical companies. DMF, acetonitrile (HPLC), and THF were purchased from Merck Chemicals. 2-Methylthiophene and 1.6 M *n*-BuLi in hexane were purchased from Alfa Aesar. Trimethylchlorosilane, (trimethylsilyl)acetylene, and octafluorocyclopentene were obtained from TCI Chemicals. Tetrakis(triphenylphosphine)-

palladium(0), used as a catalyst for Sonogashira coupling, was purchased from Sigma-Aldrich. All solvents were dried and degassed prior to use, and the reactions were performed using Schlenk techniques under a nitrogen atmosphere. The dithienylethene derivative **1**[39,40] and ferrocenyl precursor **2**[41] were prepared as previously reported. All of the solvents were either HPLC or spectroscopic grade in the optical spectroscopic studies. The reactions were monitored by thin-layer chromatography on silica gel plates, and column chromatography was conducted on a silica gel (mesh 60−120) column of 2.5 cm diameter. A conventional three-electrode configuration setup was used to perform cyclic voltammetry (CV) and differential pulse voltammetry (DPV) experiments (10^{-4} M), where glassy carbon, platinum, and silver/silver chloride (Ag/Ag^+) were used as the working electrode, auxiliary electrode, and reference electrode, respectively. Tetrabutylammonium perchlorate, $[(n\text{-}Bu_4)N]ClO_4$, was employed as the supporting electrolyte at a scan rate of 0.06 V s^{-1} for carrying out the experiments.

Preparation of the Sample for IR and Elemental Analyses of the [3o·Hg^{2+}] Complex. The pure compound **3o** was dissolved in a minimum amount of CH_3CN, to which a 1 molar equiv CH_3CN solution of $Hg(ClO_4)_2$ was added. The two solutions were mixed up progressively, and the solvent mixture was evaporated under reduced pressure. The resulting blue solid compound was washed with H_2O to remove free perchlorate anion (if any), followed by filtration by suction, and was dried under vacuum for several hours. The dry solid complex was directly used for IR and elemental analysis.

Instrumentation. ^1H and ^{13}C NMR spectroscopic measurements were recorded with a Bruker 400 MHz FT-NMR spectrometer using TMS ($SiMe_4$) as an internal reference at room temperature, and the chemical shifts are reported in ppm. The shifts were referenced to the residual solvents as follows: DMSO-d_6 2.49 ppm (^1H), CD_3CN 1.94 ppm (^1H), and $CDCl_3$ 77.15 ppm (^{13}C). HRMS were collected from a Waters HRMS Model XEVO-G2QTOF#YCA351 spectrometer. FT-IR spectra were obtained with a PerkinElmer LX-1 FT-IR spectrophotometer. UV and visible light irradiations were performed with a lamp of wavelength 365 nm. A Shimadzu-UV-1900i UV−vis spectrophotometer was used for the study of absorption spectra at room temperature. Cyclic voltammetry (CV) was performed on a CH Instruments electrochemical workstation. CHN analysis was performed on a Vario EL elementar CHNS analyzer.

***Caution!** Metal perchlorate salts are potentially explosive under certain conditions. All due precautions should be taken while handling perchlorate salts!*

Synthesis of Compound 3. An oven-dried Schlenk flask was charged with compound **1** (0.271 g, 0.5156 mmol) in distilled Et_3N solvent under a nitrogen atmosphere. The solution was further degassed by bubbling nitrogen for 45 min to remove dissolved O_2. Then the catalyst $Pd(PPh_3)_4$ (0.029 g, 0.0258 mmol) and CuI (0.006 g, 0.0361 mmol) were added under an N_2 stream. Predried solid compound **2** (0.327 g, 1.289 mmol) was added to the solution, and the reaction mixture was stirred for 7 h at 65 °C. After 7 h of stirring, the solution was cooled to room temperature and poured into H_2O. The organic layer was extracted by DCM and dried over Na_2SO_4. The residue was purified by column chromatography on silica gel (ethyl acetate/hexane 5/95) to afford the pure compound **3** (85%, yellow solid). The synthesized compound **3** was fully characterized by ^1H NMR, ^{13}C NMR, ^{19}F NMR, HRMS, IR spectroscopy and elemental analysis.

^1H NMR (400 MHz, DMSO-d_6): δ 7.31 (s, 1H, $H_{\text{thiophene}}$), 4.34 (s, 2H, OCH_2), 4.32 (s, 2H, OCH_2), 4.25 (s, 2H, H_{Cp}), 4.15 (s, 7H, H_{Cp}), 1.94 (s, 3H, CH_3). ^{13}C NMR (100 MHz, $CDCl_3$): δ 143.29 (C_{DTE}), 136.44 (C_{DTE}), 131.98 (C_{DTE}), 124.72 (C_{DTE}), 121.08 (C_{DTE}), 115.74 (C_{DTE}), 113.70 (C_{DTE}), 90.75 (C_{alkyne}), 82.21 (C_{alkyne}), 69.67 (C_{cp}), 68.83 (C_{cp}), 68.63 (C_{cp}), 68.32 (C_{cp}), 57.42 (OCH_2), 57.08 (OCH_2), 14.54 (CH_3). ^{19}F NMR (400 MHz, $CDCl_3$): δ −110.29 (s, 4F), −131.87 (s, 2F). HRMS: m/z $[M + H]^+$ calcd for $C_{43}H_{34}O_2S_2F_6Fe_2$ 873.0681; found 873.1068. Anal. Calcd for $C_{43}H_{34}O_2S_2F_6Fe_2$: C, 59.19; H, 3.93. Found: C, 60.8; H, 4.25. Anal. Calcd for $C_{43}H_{34}O_{10}S_2Cl_2F_6Fe_2Hg$ (for [**3o** + $Hg(ClO_4)_2$]): C, 40.60; H, 2.69. Found: C, 40.72; H, 2.81. IR (KBr): ν 2220.84 cm^{-1} (C≡C).

X-ray Crystallographic Analysis. Single crystals of compound **3** were grown by slow diffusion of a EtOAc/hexane (7/3 v/v) solution. Single-crystal X-ray data of compound **3o** were collected using Mo Kα (λ = 0.71069 Å) radiation at room temperature on a Microfocal D8 venture Bruker APEX 3 diffractometer equipped with a CCD area detector. The unit cell parameters were refined using all of the collected spots after the integration process. The structure was solved by direct methods and refined by full-matrix least squares on F^2 using SHELXL97.[42] All of the non-hydrogen atoms were refined with anisotropic temperature factors. Hydrogen atoms were calculated and refined in the riding mode.

Computational Details. All of the calculations (DFT and TD-DFT) were carried out utilizing the Gaussian 09 (Rev. E. 01)[43] package and were performed on a parallel cluster system. The ground-state geometries were optimized without symmetry constraints by employing the B3LYP functional,[44−46] in combination with the basis set 6-31g(d)[47,48] for all nonmetallic atoms (C, H, O, F, S, and Cl) and the double-ξ-quality basis set LANL2DZ[49,50] for the metal atoms (Fe and Hg). The optimized geometries were confirmed to be local minima by performing frequency calculations and obtaining only positive (real) frequencies. The zero-point-corrected energy values are reported herein. On the basis of the optimized structures, the lowest-energy vertical transitions were calculated (singlets, 15 states) by TD-DFT, using the Coulomb-attenuated functional CAM-B3LYP[51] at the aforementioned level of calculation. All of the calculations (geometry optimizations and frequency calculations, MO calculations, TDDFT) have been performed including solvent effects through the polarizable continuum model (PCM) that uses the integral equation formalism variant (IEFPCM).

■ ASSOCIATED CONTENT

Supporting Information

The Supporting Information is available free of charge at https://pubs.acs.org/doi/10.1021/acs.inorgchem.1c00602.

Experimental details, NMR spectra, XRD data, photophysical and electrochemical studies, and additional theoretical data (PDF)

Accession Codes

CCDC 2039561 contains the supplementary crystallographic data for this paper. These data can be obtained free of charge via www.ccdc.cam.ac.uk/data_request/cif, or by emailing data_request@ccdc.cam.ac.uk, or by contacting The Cambridge Crystallographic Data Centre, 12 Union Road, Cambridge CB2 1EZ, UK; fax: +44 1223 336033.

■ AUTHOR INFORMATION

Corresponding Author

Arunabha Thakur − *Department of Chemistry, Jadavpur University, Kolkata 700032, India;* orcid.org/0000-0003-4577-3683; Phone: +919937760940; Email: arunabha.thakur@jadavpuruniversity.in, babuiitm07@gmail.com

Authors

Manisha Karmakar − *Department of Chemistry, Jadavpur University, Kolkata 700032, India*

Adwitiya Pal − *Department of Chemistry, Jadavpur University, Kolkata 700032, India*

Bijan Mondal − *Institut für Anorganische Chemie, Universität Regensburg, 93040 Regensburg, Germany;* orcid.org/0000-0002-7359-8926

Nayarassery N. Adarsh − *Solid State and Materials Chemistry Research Group, School of Chemical Sciences, Mahatma*

Gandhi University, Kerala 686560, India; orcid.org/0000-0003-2262-8512

Complete contact information is available at:
https://pubs.acs.org/10.1021/acs.inorgchem.1c00602

Notes

The authors declare no competing financial interest.

■ ACKNOWLEDGMENTS

M.K. and A.P. are thankful to the STATE and CSIR for JRF fellowships, respectively. The authors acknowledge a UGC start up grant (30-421/2018/BSR) for financial support.

■ REFERENCES

(1) Wigglesworth, T. J.; Branda, N. R. A family of multiaddressable, multicolored photoresponsive copolymers prepared by ring-opening metathesis polymerization. *Chem. Mater.* **2005**, *17*, 5473−5480.

(2) Baggaley, E.; Botchway, S. W.; Haycock, J. W.; Morris, H.; Sazanovich, I. V.; Williams, J. A. G.; Weinstein, J. A. Long-lived metal complexes open up microsecond lifetime imaging microscopy under multiphoton excitation: From FLIM to PLIM and beyond. *Chem. Sci.* **2014**, *5*, 879−886.

(3) (a) Kobatake, S.; Yamada, T.; Uchida, K.; Kato, N.; Irie, M. Photochromism of 1,2-Bis(2,5-dimethyl-3-thienyl)perfluoro-cyclopentene in a single crystalline phase. *J. Am. Chem. Soc.* **1999**, *121*, 2380−2386. (b) Irie, M.; Mohri, M. Thermally irreversible photochromic systems. Reversible photocyclization of diarylethene derivatives. *J. Org. Chem.* **1988**, *53*, 803−808. (c) Irie, M.; Sakemura, K.; Okinaka, M.; Uchida, K. Photochromism of dithienylethenes with electron-donating substituents. *J. Org. Chem.* **1995**, *60*, 8305−8309.

(4) Li, R.; Nakashima, T.; Galangau, O.; Iijima, S.; Kanazawa, R.; Kawai, T. Photon-quantitative 6π-electrocyclization of a diarylbenzo[b]thiophene in polar medium. *Chem. - Asian J.* **2015**, *10*, 1725−1730.

(5) (a) Guerchais, V.; Ordronneau, L.; Bozec, H. L. Recent developments in the field of metal complexes containing photochromic ligands: Modulation of linear and nonlinear optical properties. *Coord. Chem. Rev.* **2010**, *254*, 2533−2545. (b) Shen, C.; He, X.; Toupet, L.; Norel, L.; Rigaut, S.; Crassous, J. Dual redox and optical control of chiroptical activity in photochromic dithienylethenes decorated with hexahelicene and bis-ethynyl-ruthenium units. *Organometallics* **2018**, *37*, 697−705. (c) Ordronneau, L.; Aubert, V.; Guerchais, V.; Boucekkine, A.; Bozec, H. L.; Singh, A.; Ledoux, I.; Jacquemin, D. The first hexadithienylethene-substituted tris(bipyridine) metal complexes as quadratic NLO photoswitches: Combined experimental and DFT studies. *Chem. Eur. J.* **2013**, *19*, 5845−5849.

(6) (a) Sun, C.-L.; Gao, Z.; Teng, K.-X.; Niu, L.-Y.; Chen, Y.-Z.; Zhao, Y. S.; Yang, Q.-Z. Supramolecular polymer-based fluorescent microfibers for switchable optical waveguides. *ACS Appl. Mater. Interfaces* **2018**, *10*, 26526−26532. (b) Wigglesworth, T. J.; Myles, A. J.; Branda, N. R. High-content photochromic polymers based on dithienylethenes. *Eur. J. Org. Chem.* **2005**, 1233−1238.

(7) Pärs, M.; Hofmann, C. C.; Willinger, K.; Bauer, P.; Thelakkat, M.; Köhler, J. An organic optical transistor operated under ambient conditions. *Angew. Chem., Int. Ed.* **2011**, *50*, 11405−11408.

(8) (a) Boixel, J.; Guerchais, V.; Bozec, H. L.; Jacquemin, D.; Amar, A.; Boucekkine, A.; Colombo, C.; Dragonetti, A.; Marinotto, D.; Roberto, D.; Righetto, S.; Angelis, R. D. Second-order NLO switches from molecules to polymer films based on photochromic cyclometalated platinum(II) complexes. *J. Am. Chem. Soc.* **2014**, *136*, 5367−5375. (b) Ordronneau, L.; Nitadori, H.; Ledoux, I.; Singh, A.; Williams, J. A. G.; Akita, M.; Guerchais, V.; Bozec, H. L. Photochromic metal complexes: Photoregulation of both the nonlinear optical and luminescent properties. *Inorg. Chem.* **2012**, *51*, 5627−5636. (c) Ma, T. Y.; Ma, N. N.; Yan, L. K.; Zhang, T.; Su, Z. M. Theoretical exploration of photoisomerization-switchable second-order nonlinear optical responses of two-dimendional Λ- and W-shaped polyoxometalate derivatives of dithienylperfluorocyclopentene. *J. Phys. Chem. A* **2013**, *117*, 10783−10789.

(9) Monaco, S.; Semeraro, M.; Tan, W.; Tian, H.; Ceroni, P.; Credi, A. Multifunctional switching of a photo- and electro-chemiluminescent iridium-dithienylethene complex. *Chem. Commun.* **2012**, *48*, 8652−8654.

(10) Green, K. A.; Cifuentes, M. P.; Corkery, T. C.; Samoc, M.; Humphrey, M. G. Switching the cubic nonlinear optical properties of an electro-, halo-, and photochromic ruthenium alkynyl complex across six states. *Angew. Chem., Int. Ed.* **2009**, *48*, 7867−7870.

(11) Aubert, V.; Guerchais, V.; Ishow, E.; Hoang-Thi, K.; Ledoux, I.; Nakatani, K.; Bozec, H. L. Efficient photoswitching of the nonlinear optical properties of dipolar photochromic zinc(II) complexes. *Angew. Chem., Int. Ed.* **2008**, *47*, 577−580.

(12) Nitadori, H.; Ordronneau, L.; Boixel, J.; Jacquemin, D.; Boucekkine, A.; Singh, A.; Akita, M.; Ledoux, I.; Guerchais, V.; Bozec, H. L. Photoswitching of the second-order nonlinearity of a tetrahedral octupolar multi DTE-based copper(I) complex. *Chem. Commun.* **2012**, *48*, 10395−10397.

(13) Roberts, M. N.; Nagle, J. K.; Majewski, M. B.; Finden, J. G.; Branda, N. R.; Wolf, M. O. Charge transfer and intraligand excited state interactions in platinum-sensitized dithienylethenes. *Inorg. Chem.* **2011**, *50*, 4956−4966.

(14) (a) Li, R.-J.; Holstein, J. J.; Hiller, W. G.; Andréasson, J.; Clever, G. H. Mechanistic interplay between light switching and guest binding in photochromic [Pd_2Dithienylethene$_4$] coordination cages. *J. Am. Chem. Soc.* **2019**, *141*, 2097−2103. (b) Han, M.; Luo, Y.; Damaschke, B.; Gómez, L.; Ribas, X.; Jose, A.; Peretzki, P.; Seibt, M.; Clever, G. H. Light-controlled interconversion between a self-assembled triangle and a rhombicuboctahedral sphere. *Angew. Chem., Int. Ed.* **2016**, *55*, 445−449. (c) Li, R.-J.; Han, M.; Tessarolo, J.; Holstein, J. J.; Lübben, J.; Dittrich, B.; Volkmann, C.; Finze, M.; Jenne, C.; Clever, G. H. Successive photoswitching and derivatization effects in photochromic dithienylethene-based coordination cages. *ChemPhotoChem* **2019**, *3*, 378−383. (d) Han, M.; Michel, R.; He, B.; Chen, Y.-S.; Stalke, D.; John, M.; Clever, G. H. Light-triggered guest uptake and release by a photochromic coordination cage. *Angew. Chem., Int. Ed.* **2013**, *52*, 1319−1323.

(15) Piao, X.; Zou, Y.; Wu, J.; Li, C.; Yi, T. Multiresponsive switchable diarylethene and its application in bioimaging. *Org. Lett.* **2009**, *11*, 3818−3821.

(16) (a) Qiu, S.; Cui, S.; Shi, F.; Pu, S. Novel diarylethene-based fluorescent switching for the detection of Al^{3+} and construction of logic circuit. *ACS Omega* **2019**, *4*, 14841−14848. (b) Feng, E.; Fan, C.; Wang, N.; Liu, G.; Pu, S. A highly selective diarylethene chemosensor for colorimetric detection of CN^- and fluorescent relay-detection of Al^{3+}/Cr^{3+}. *Dyes Pigm.* **2018**, *151*, 22−27. (c) Jing, S.; Zheng, C.; Pu, S.; Fan, C.; Liu, G. A highly selective ratiometric fluorescent chemosensor for Hg^{2+} based on a new diarylethene with a stilbene-linked terpyridine unit. *Dyes Pigm.* **2014**, *107*, 38−44.

(17) Wang, Q.; Yu, C.; Zhang, C.; Long, H.; Azarnoush, S.; Jin, Y.; Zhang, W. Dynamic covalent synthesis of aryleneethynylene cages through alkyne metathesis: Dimer, tetramer, or interlocked complex? *Chem. Sci.* **2016**, *7*, 3370−3376.

(18) Sánchez, R. S.; Gras-Charles, R.; Bourdelande, J. L.; Guirado, G.; Hernando, J. Light- and redox-controlled fluorescent switch based on a perylenediimide-dithienylethene dyad. *J. Phys. Chem. C* **2012**, *116*, 7164−7172.

(19) (a) Motoyama, K.; Li, H.; Koike, T.; Hatakeyama, M.; Yokojima, S.; Nakamura, S.; Akita, M. Photo- and electro-chromic organometallics with dithienylethene (DTE) linker, L_2CpM-DTE-MCpL_2: Dually stimuli-responsive molecular switch. *Dalton Trans.* **2011**, *40*, 10643−10657. (b) Li, B.; Wang, J.-Y.; Wen, H.-M.; Shi, L.-X.; Chen, Z.-N. Redox-modulated stepwise photochromism in a ruthenium complex with dual dithienylethene-acetylides. *J. Am. Chem. Soc.* **2012**, *134*, 16059−16067.

(20) (a) Li, B.; Wen, H.-M.; Wang, J.-Y.; Shi, L.-X.; Chen, Z.-N. Modulating stepwise photochromism in platinum(II) complexes with

dual dithienylethene-acetylides by a progressive red shift of ring-closure absorption. *Inorg. Chem.* **2013**, *52*, 12511−12520. (b) Matsuda, K.; Takayama, K.; Irie, M. Single-crystalline photochromism of a linear coordination polymer composed of 1,2-bis[2-methyl-5-(4-pyridyl)-3-thienyl]perfluorocyclopentene and bis-(hexafluoroacetylacetonato)zinc(II). *Chem. Commun.* **2001**, 363−364.

(21) Guirado, G.; Coudret, C.; Launay, J.-P. Electrochemical remote control for dithienylethene-ferrocene switches. *J. Phys. Chem. C* **2007**, *111*, 2770−2776.

(22) Zhao, H.; Garoni, E.; Roisnel, T.; Colombo, A.; Dragonetti, C.; Marinotto, D.; Righetto, S.; Roberto, D.; Jacquemin, D.; Boixel, J.; Guerchais, V. Photochromic DTE-substituted-1,3-di(2-pyridyl)-benzene platinum(II) complexes: Photomodulation of luminescence and second-order nonlinear optical properties. *Inorg. Chem.* **2018**, *57*, 7051−7063.

(23) Boixel, J.; Guerchais, V.; Bozec, H. L.; Chantzis, A.; Jacquemin, D.; Colombo, A.; Dragonetti, C.; Marinottoe, D.; Roberto, D. Sequential double second-order nonlinear optical switch by an acido-triggered photochromic cyclometallated platinum(II) complex. *Chem. Commun.* **2015**, *51*, 7805−7808.

(24) (a) Lloveras, V.; Caballero, A.; Tárraga, A.; Velasco, M. D.; Espinosa, A.; Wurst, K.; Evans, D. J.; Vidal-Gancedo, J.; Rovira, C.; Molina, P.; Veciana, J. Synthesis and characterization of radical cations derived from mono- and biferrocenyl-substituted 2-aza-1,3-butadienes: A study of the influence of an asymmetric and oxidizable bridge on intramolecular electron transfer. *Eur. J. Inorg. Chem.* **2005**, 2436−2450. (b) Zhao, L.; Ling, Q.; Liu, X.; Hang, C.; Zhao, Q.; Liu, F.; Gu, H. Multifunctional triazolylferrocenyl Janus dendron: Nanoparticle stabilizer, smart drug carrier and supramolecular nanoreactor. *Appl. Organomet. Chem.* **2018**, *32*, 4000−4012.

(25) Remón, P.; González, D.; Li, S.; Basílio, N.; Andréasson, J.; Pischel, U. Light-driven control of the composition of a supramolecular network. *Chem. Commun.* **2019**, *55*, 4335−4338.

(26) (a) Irie, M.; Lifka, T.; Kobatake, S.; Kato, N. Photochromism of 1,2-Bis(2-methyl-5-phenyl-3-thienyl)perfluorocyclopentene in a single-crystalline phase. *J. Am. Chem. Soc.* **2000**, *122*, 4871−4876. (b) Tanaka, Y.; Ishisaka, T.; Inagaki, A.; Koike, T.; Lapinte, C.; Akita, M. Photochromic organometallics with a dithienylethene (DTE) bridge, [Y-C≡C-DTE-C≡C-Y] (Y = {MCp*(dppe)}): Photoswitchable molecular wire (M = Fe) versus dual photo- and electrochromism (M = Ru). *Chem. Eur. J.* **2010**, *16*, 4762−4776.

(27) Wan, H.; Xue, H.; Ling, Y.; Qiao, Y.; Chen, Y.; Zhou, G. Electron donor and acceptor functionalized dithienylethenes: Effects of charge density on photochromic properties. *Phys. Chem. Chem. Phys.* **2018**, *20*, 14348−14356.

(28) Karmakar, M.; Bhatta, S. R.; Giri, S.; Thakur, A. Oxidation-induced differentially selective turn-on fluorescence *via* photoinduced electron transfer based on a ferrocene-appended coumarin-quinoline platform: Application in cascaded molecular logic. *Inorg. Chem.* **2020**, *59*, 4493−4507.

(29) Harvey, E. C.; Areephong, J.; Cafolla, A. A.; Long, C.; Browne, W. R.; Feringa, B. L.; Pryce, M. T. Incorporating cobalt carbonyl moieties onto ethynylthiophene- based dithienylcyclopentene switches. 2. Electro- and spectroelectrochemical properties. *Organometallics* **2014**, *33*, 3309−3319.

(30) Otón, F.; Tárraga, A.; Molina, P. A bis-guanidine-based multisignaling sensor molecule that displays redox-ratiometric behavior or fluorescence enhancement in the presence of anions and cations. *Org. Lett.* **2006**, *8*, 2107−2110.

(31) Zhong, Y.-W.; Vila, N.; Henderson, J. C.; Abruña, H. D. Dithienylcyclopentenes-containing transition metal bisterpyridine complexes directed toward molecular electronic applications. *Inorg. Chem.* **2009**, *48*, 991−999.

(32) Liu, Y.; Ndiaye, C. M.; Lagrost, C.; Costuas, K.; Choua, S.; Turek, P.; Norel, L.; Rigaut, S. Diarylethene-containing carbon-rich ruthenium organometallics: Tuning of electrochromism. *Inorg. Chem.* **2014**, *53*, 8172−8188.

(33) Hatai, J.; Pal, S.; Jose, G. P.; Bandyopadhyay, S. Histidine based fluorescence sensor detects Hg^{2+} in solution, paper strips, and in cells. *Inorg. Chem.* **2012**, *51*, 10129−10135.

(34) The upfield shift of methyl protons is due to the close proximity to the coordination site, as reported in: Lin, Y.; Jiang, C.; Hu, F.; Yin, J.; Yu, G.-A.; Liu, S. H. Synthesis, characterization, and properties of some bisacetylide and binuclear acetylide gold(I) compounds based on the photochromic dithienylethene unit. *Dyes Pigm.* **2013**, *99*, 995−1003.

(35) Chen, Y.; Zhang, Y.-H.; Zhao, L.-J. ATR-FTIR spectroscopic studies on aqueous $LiClO_4$, $NaClO_4$, and $Mg(ClO_4)_2$ solutions. *Phys. Chem. Chem. Phys.* **2004**, *6*, 537−542.

(36) (a) Perrier, A.; Maurel, F.; Aubard, J. Theoretical investigation of the substituent effect on the electronic and optical properties of photochromic dithienylethene derivatives. *J. Photochem. Photobiol., A* **2007**, *189*, 167−176. (b) Perrier, A.; Maurel, F.; Jacquemin, D. Interplay between electronic and steric effects in multiphotochromic diarylethenes. *J. Phys. Chem. C* **2011**, *115*, 9193−9203.

(37) A previous report showed that a distance of 1.53 Å is required for the molecule to be thermodynamically stable. See: (a) Maurel, F.; Perrier, A.; Perpète, E. A.; Jacquemin, D. A theoretical study of the perfluoro-diarylethenes electronic spectra. *J. Photochem. Photobiol., A* **2008**, *199*, 211−223. (b) Perrier, A.; Maurel, F.; Jacquemin, D. Single molecule multiphotochromism with diarylethenes. *Acc. Chem. Res.* **2012**, *45*, 1173−1182. (c) Boixel, J.; Zhu, Y.; Bozec, H. L.; Benmensour, M. A.; Boucekkine, A.; Wong, K. M. -C.; Colombo, A.; Roberto, D.; Guerchais, V.; Jacquemin, D. Contrasted photochromic and luminescent properties in dinuclear Pt(II) complexes linked through a central dithienylethene unit. *Chem. Commun.* **2016**, *52*, 9833−9836.

(38) (a) Manceau, A.; Lemouchi, C.; Rovezzi, M.; Lanson, M.; Glatzel, P.; Nagy, K. L.; Gautier-Luneau, I.; Joly, Y.; Enescu, M. Structure, bonding, and stability of mercury complexes with thiolate and thioether ligands from high-resolution XANES spectroscopy and first-principles calculations. *Inorg. Chem.* **2015**, *54*, 11776−11791. (b) Li, X.; Liao, R.-Z.; Zhou, W.; Chen, G. DFT studies of the degradation mechanism of methyl mercury activated by a sulfur-rich ligand. *Phys. Chem. Chem. Phys.* **2010**, *12*, 3961−3971.

(39) Zhang, N.; Lo, W.-Y.; Jose, A.; Cai, Z.; Li, L.; Yu, L. A single-molecular AND gate operated with two orthogonal switching mechanisms. *Adv. Mater.* **2017**, *29*, 1701248.

(40) Fredrich, S.; Bonasera, A.; Valderrey, V.; Hecht, S. Sensitive assays by nucleophile-induced rearrangement of photoactivated diarylethenes. *J. Am. Chem. Soc.* **2018**, *140*, 6432−6440.

(41) Bhatta, S. R.; Bheemireddy, V.; Thakur, A. A redox-driven fluorescence "Off-On" molecular switch based on a 1,1′-unsymmetrically substituted ferrocenyl coumarin system: Mimicking combinational logic operation. *Organometallics* **2017**, *36*, 829−838.

(42) Sheldrick, G. M. A short history of SHELX. *Acta Crystallogr., Sect. A: Found. Crystallogr.* **2008**, *64*, 112−122.

(43) Frisch, M. J.; Trucks, G. W.; Schlegel, H. B.; Scuseria, G. E.; Robb, M. A.; Cheeseman, J. R.; Scalmani, G.; Barone, V.; Mennucci, B.; Petersson, G. A.; Nakatsuji, H.; Caricato, M.; Li, X.; Hratchian, H. P.; Izmaylov, A. F.; Bloino, J.; Zheng, G.; Sonnenberg, J. L.; Hada, M.; Ehara, M.; Toyota, K.; Fukuda, R.; Hasegawa, J.; Ishida, M.; Nakajima, T.; Honda, Y.; Kitao, O.; Nakai, H.; Vreven, T.; Montgomery, J. A.; Peralta, J. E.; Ogliaro, F.; Bearpark, M.; Heyd, J. J.; Brothers, E.; Kudin, K. N.; Staroverov, V. N.; Keith, T.; Kobayashi, R.; Normand, J.; Raghavachari, K.; Rendell, A.; Burant, J. C.; Iyengar, S. S.; Tomasi, J.; Cossi, M.; Rega, N.; Millam, J. M.; Klene, M.; Knox, J. E.; Cross, J. B.; Bakken, V.; Adamo, C.; Jaramillo, J.; Gomperts, R.; Stratmann, R. E.; Yazyev, O.; Austin, A. J.; Cammi, R.; Pomelli, C.; Ochterski, J. W.; Martin, R. L.; Morokuma, K.; Zakrzewski, V. G.; Voth, G. A.; Salvador, P.; Dannenberg, J. J.; Dapprich, S.; Daniels, A. D.; Farkas, O.; Foresman, J. B.; Ortiz, J. V.; Cioslowski, J.; Fox, D. J. *Gaussian 09, Rev. E.01*; Gaussian, Inc.: Wallingford, CT, 2013.

(44) Becke, A. D. Density functional thermochemistry. III. The role of exact exchange. *J. Chem. Phys.* **1993**, *98*, 5648−5652.

(45) Lee, C.; Yang, W.; Parr, R. G. Development of the colle-salvetti correlation-energy formula into a functional of the electron density. *Phys. Rev. B: Condens. Matter Mater. Phys.* **1988**, *37*, 785−789.

(46) Stephens, P. J.; Devlin, F. J.; Chabalowski, C. F.; Frisch, M. J. Ab Initio calculation of vibrational absorption and circular dichroism spectra using density functional force fields. *J. Phys. Chem.* **1994**, *98*, 11623−11627.

(47) Petersson, G. A.; Al-Laham, M. A. A complete basis set model chemistry. II. Open-shell systems and the total energies of the first-row atoms. *J. Chem. Phys.* **1991**, *94*, 6081−6090.

(48) Petersson, G. A.; Bennett, A.; Tensfeldt, T. G.; Al-Laham, M. A.; Shirley, W. A.; Mantzaris, J. A complete basis set model chemistry. I. The total energies of closed-shell atoms and hydrides of the first-row elements. *J. Chem. Phys.* **1988**, *89*, 2193−2218.

(49) Wadt, W. R.; Hay, P. J. Ab initio effective core potentials for molecular calculations. Potentials for main group elements Na to Bi. *J. Chem. Phys.* **1985**, *82*, 284−298.

(50) Hay, P. J.; Wadt, W. R. Ab initio effective core potentials for molecular calculations. Potentials for K to Au including the outermost core orbitals. *J. Chem. Phys.* **1985**, *82*, 299−310.

(51) Yanai, T.; Tew, D. P.; Handy, N. C. A new hybrid exchange-correlation functional using the Coulomb-attenuating method (CAM-B3LYP). *Chem. Phys. Lett.* **2004**, *393*, 51−57.